Plant Science 303 (2021) 110774

Contents lists available at ScienceDirect

Plant Science

journal homepage: www.elsevier.com/locate/plantsci

H_2O_2 priming promotes salt tolerance in maize by protecting chloroplasts ultrastructure and primary metabolites modulation

Gyedre dos Santos Araújo [a], Stelamaris de Oliveira Paula-Marinho [a], Sergimar Kennedy de Paiva Pinheiro [b], Emílio de Castro Miguel [b], Lineker de Sousa Lopes [a], Elton Camelo Marques [a], Humberto Henrique de Carvalho [a], Enéas Gomes-Filho [c,*]

[a] Department of Biochemistry and Molecular Biology, Federal University of Ceará, Brazil
[b] Department of Metallurgical and Materials Engineering and Analytical Center, Federal University of Ceará, Fortaleza, Brazil
[c] Department of Biochemistry and Molecular Biology and National Institute of Science and Technology in Salinity (INCTSal/CNPq), Federal University of Ceará, Pici Campus St., 60455-760, Fortaleza, CE, Brazil

ARTICLE INFO

Keywords:
Acclimation
Metabolomic
Photosynthesis
Salt stress
Zea mays

ABSTRACT

Hydrogen peroxide priming has emerged as a powerful strategy to trigger multiple responses involved in plant acclimation that reinforce tolerance to abiotic stresses, including salt stress. Thus, this study aimed to investigate the impact of foliar H_2O_2 priming on the physiological, biochemical, and ultrastructural traits related to photosynthesis of salt-stressed plants. Besides, we provided comparative leaf metabolomic profiles of *Zea mays* plants under such conditions. For this, H_2O or H_2O_2 pretreated plants were grown under saline conditions for 12-days. Salinity drastically affected photosynthetic parameters and structural chloroplasts integrity, also increased reactive oxygen species contents promoting disturbance in the plant metabolism when compared to non-saline conditions. Our results suggest that H_2O_2-pretreated plants improved photosynthetic performance avoiding salinity-induced energy excess and ultrastructural damage by preserving stacking thylakoids. It displayed modulation of some metabolites, as arabitol, glucose, asparagine, and tyrosine, which may contribute to the maintenance of osmotic balance and reduced oxidative stress. Hence, our study brings new insights into an understanding of plant acclimation to salinity by H_2O_2 priming based on photosynthesis maintenance and metabolite modulation.

1. Introduction

Maize (*Zea mays* L.) plants have been one of the most energy sources for human and animal nutrition in the world [1,2]. Nevertheless, maize growth and quality of grains can be severely affected by salinity, drought, high temperatures, among other adverse environmental conditions [3] that are responsible for a yield reduction of over 50 % in major global crops [4]. Salinity has a notable negative impact on crops worldwide, in which physiological, biochemical, morphological, and molecular processes are impaired by osmotic stress and ionic toxicity generated by salinity, leading to a series of secondary stresses, including oxidative burst [5,6]. Salinity directly affects the integrity of chloroplast ultrastructure and causes lamellar disorders, affecting photosynthesis processes [7]. It can additionally reduce the content of photosynthetic pigments and electron transport in the thylakoid membrane [8,9]. Salt stress also can alter the activity of carbon-fixing enzymes and the regulation of plant metabolism [10]. That way, efficient acclimation to salt stress includes several structural or molecular changes. Also, the priming technique can be a helpful tool to reach acclimation inducing molecular mechanisms associated with salt tolerance in plant crops [11–13].

Overall, the priming can be achieved by pretreatment with synthetic

Abbreviations: *A*, CO_2 assimilation; *A/Ci*, carboxylation efficiency; Car, carotenoids; Chl, chlorophyll; *E*, transpiration; ETR, electron transport rate; Fv/Fm, maximum quantum yield of photosystem II; g_s, stomatal conductance; NPQ, non-photochemical quenching; PEPcase, phosphoenolpyruvate carboxylase; qP, photochemical quenching; ΦPSII, effective quantum yield of photosystem II; Ψs, osmotic potential.

* Corresponding author.
E-mail addresses: gyedrearaujo@yahoo.com.br (G. dos Santos Araújo), maris.biologa@gmail.com (S. de Oliveira Paula-Marinho), sergimarkennedy@hotmail.com (S.K. de Paiva Pinheiro), emilio@centralanalitica.ufc.br (E. de Castro Miguel), linekerlk@gmail.com (L. de Sousa Lopes), bioelton12@yahoo.com.br (E. Camelo Marques), humberto.carvalho@ufc.br (H.H. de Carvalho), egomesf@ufc.br (E. Gomes-Filho).

https://doi.org/10.1016/j.plantsci.2020.110774
Received 11 August 2020; Received in revised form 19 October 2020; Accepted 24 November 2020
Available online 28 November 2020

or natural compounds as H_2O_2 applied on seed, root, or leaves [14,15]. The H_2O_2 is one of the reactive oxygen species (ROS) produced during cell metabolism; at low levels, it functions as a signaling agent, but in excess generates oxidative stress in plant cells, which usually occurs under severe environmental stresses [16]. The linkage of H_2O_2 and abiotic stress in the intracellular signaling for physiological responses remain not entirely clear, bearing in mind that the acclimation responses depend on specific ROS signatures to tailor plant to the stress encounters it [5]. Meanwhile, a promising improvement in photosynthesis by H_2O_2 priming can be related to carbon fixation enzymes activity, PSII efficiency, and protection of cellular organelles, such as chloroplasts [17,18]. Also, previous studies have demonstrated that application exogenous of a 10 mM H_2O_2 solution as a priming agent in maize leaves confers tolerance to salt stress [19,20]. This H_2O_2 priming modulated various cellular processes associated with high antioxidant enzyme activities and increased soluble protein and soluble carbohydrates contents too.

Over the last years, the untargeted plant metabolomics has risen as a powerful research tool to study mechanisms of stress tolerance mainly because of the different modulate compounds [21,22]. Although an overall metabolic reprogramming occurs in plants exposed to abiotic stresses, it is quite different among species. Some species synthesize and accumulate low quantities of specific metabolites, whereas some others do not do so at all [10,23]. Thus, it becomes relevant to understand the metabolic reprogramming of primed plants under stress, accessing the primary metabolism and its relationship with other physiological responses. Given the economic importance of maize and its relative sensitivity to salinity, a better understanding regarding salt tolerance by H_2O_2 priming becomes especially pertinent. Our purpose was to investigate if salt tolerance induced by H_2O_2 exogenous reported in maize by other studies be the result of regulation and upkeep of photosynthetic machinery coupled with positive modulation of key metabolites as carbohydrates.

2. Material and methods

2.1. Plant material and experimental conditions

The maize (*Zea mays* L.) cultivar was BR 5011, considered sensitive to salinity [24]. The seeds surfaces were sanitized in a 1 % NaClO solution for 10 min before sown. After seven days of sowing, uniform seedlings were transferred to 10-L trays containing half-strength Hoagland's nutrient solution [25] for five days, as an acclimation time. Then, 15 mL plant^{-1} of 10 mM H_2O_2 solution or an equal volume of distilled water was sprayed directly on the leaves, both containing 0.025 % Tween 20 detergent, to break water surface tension, facilitating H_2O_2 diffusion into mesophyll cells. The application with a 10 mM H_2O_2 solution was defined based on previous studies with promising results [19]. This pretreatment was performed around 6:00 am and repeated the next day. Two days after the priming end, the plants were transferred to a 6-L plastic pot containing half-strength Hoagland's nutrient solution without and with saline treatment. The saline treatment (80 mM NaCl) was first applied in two installments to avoid osmotic shock, so the NaCl concentration was increased daily by 40 mM until the desired level. After that, the 80 mM NaCl treatment was applied in its entirety to each solution change. All nutrient solutions were renewed every four days, and the pH was maintained between 5.5 and 6.0. The experiments were conducted in a greenhouse located in the tropical semiarid region of Northeastern Brazil under average values of temperature, relative humidity, and photosynthetic photon flux density (PPFD) of 32.3 °C, 44.8 %, and 1,050 µmol photon m^{-2} s^{-1}, respectively. The plants were kept under twelve days of salt stress. At the end of the experiment, they were harvested and grouped into four treatments according to growth conditions: water-pretreated (1) and H_2O_2-pretreated (2) plants both under non-salt conditions, and water-pretreated (3) and H_2O_2-pretreated (4) plants both under salt stress.

2.2. Gas exchange and chlorophyll *a* fluorescence

The gas exchange and chlorophyll *a* fluorescence were performed in the middle third of the fully expanded leaves under constant CO_2 concentration and PPFD of 400 µmol mol^{-1} CO_2 and 1,200 µmol photons m^{-2} s^{-1}, respectively. Two measurements were performed by repetition, and the chamber size used was 2 cm^2. Rates of CO_2 assimilation (*A*), transpiration (*E*), stomatal conductance (g_s), and carboxylation efficiency (*A/Ci*) were measured employing a portable photosynthetic system (IRGA, mod. LI-6400XT, LI-COR, Lincoln, USA) coupled with artificial light. The chlorophyll *a* fluorescence parameters [maximum (Fm) and variable (Fv) fluorescence in dark-adapted leaves, maximum (Fm') and dynamic (Fs) equilibrium state in the presence of light, and basal fluorescence (Fo') after excitation state of photosystem I] were measured using a fluorometer (6400-40, LI-COR, USA) coupled to IRGA. From the chlorophyll *a* fluorescence, the following photochemical parameters were estimated: maximum quantum yield of PSII [Fv/Fm = (Fm - Fo)/Fm], effective quantum yield of PSII [ΦPSII = (Fm' - Fs)/Fm'], photochemical [qP = (Fm' - Fs)/(Fm' - Fo')] and non-photochemical [NPQ = (Fm - Fm')/Fm'] quenching, and electron transport rate (ETR = ΦPSII x PPFD x 0.5 x 0.84) [26].

2.3. Measurement of osmotic potential

For determination of osmotic potential (Ψs), the sap was extracted from 350 mg of maize leaves expanded newly harvested by pressing the plant material with the aid of a disposable syringe. Then the obtained liquid (extract) was centrifuged at 6,000 *g* for 5 min, and the supernatant used to determine the Ψs using the osmometer (VAPRO 5520, Wescor, Utah, USA) [27].

2.4. Photosynthetic pigments contents

Contents of chlorophyll *a* (Chl *a*), *b* (Chl *b*), and total (Chl *total*), and carotenoids (Car) were determined from leaf discs of 1 cm^2, a total fresh mass of approximately 0.25 g, obtained from the middle third of fully expanded leaves. For pigments extraction, tubes containing the leaf discs were incubating in dimethyl sulfoxide saturated with $CaCO_3$, during 48 h at room temperature. After, the tubes were kept in the dark for 24 h and then incubated in a 65 °C water bath for 30 min. Photosynthetic pigments were spectrophotometrically measured by reading the absorbance at A_{480}, A_{649}, and A_{665}. The concentrations were calculated through the following equations: Chl $a = 12.47A_{665} - 3.62A_{649}$, Chl $b = 25.06A_{649} - 6.50A_{665}$, Chl *total* $= 7.15A_{665} + 18.71A_{649}$, and Car = $(1000A_{480} - 1.29$ Chl $a - 53.78$ Chl $b)/220$ [28].

2.5. ROS contents

The leaf extracts used for the determination of H_2O_2 contents were prepared according to methods of Cheeseman [29], with some modifications. Approximately 0.5 g of fresh tissue from fully expanded leaves was macerated with liquid nitrogen, followed by homogenization at 4 °C with 100 mM potassium phosphate buffer solution, pH 6.3. The homogenate was centrifuged at 12,000*g* at 4 °C for 15 min, and the supernatant immediately evaluated. The reaction for H_2O_2 determination consisted of 350 µL plant extract; 350 µL 12 mM phenol; 100 µL 0.5 mM 4-aminoantipyrine; 350 µL 84 mM phosphate buffer (pH 7.0) and 40 µL 1 U mL^{-1} HRP (horseradish peroxidase) diluted in 100 mM phosphate buffer pH 6.0. The reaction mixture was shaken and heated at 37 °C for 30 min. The H_2O_2 concentration of the reaction medium was determined by reading at 505 nm and comparing with a standard curve obtained from increasing H_2O_2 concentrations as standard according to method of Fernando and Soysa [30].

The determination of superoxide radical ($^{\bullet}O_2^-$) content was performed according to Klein et al. [31], with some modifications. The fresh leaf tissue (0.25 g) macerated in liquid nitrogen was homogenized at

4 °C in 65 mM potassium phosphate buffer pH 7.8. The homogenate was centrifuged at 10,000*g* for 10 min at 4 °C, and the supernatant used immediately. The reaction occurred by the addition of 250 μL extract to a mixture composed of 65 mM phosphate buffer (pH 7.8) and 50 μL 10 mM hydroxylamine. The tubes were shaken and incubated at 25 °C for one hour. Next, 1000 μL of the mixture from 58 mM sulfanilamide and 7 mM N-naphthyl ethylenediamine (1:1) were added. Finally, 1000 μL ethyl ether was added to the tubes. The $^{\bullet}O_2^-$ concentration was determined by absorbance of pink aqueous phase at 530 nm and based on a standard curve obtained from increasing $NaNO_2$ concentrations.

2.6. Phosphoenolpyruvate carboxylase activity

Extracts for determination of phosphoenolpyruvate carboxylase activity (PEPcase, EC 4.1.1.31) were prepared according to Echevarria et al. [32], with some modifications. Initially, approximately 0.25 g of fresh material from fully expanded leaves were macerated with liquid nitrogen and homogenized with 1.0 mL 100 mM Tris−HCl buffer (pH 7.5) containing 5 % glycerol, 10 mM $MgCl_2$, 1.0 mM EDTA, 1.0 mM Na_3VO_4, 5.0 mM dithiothreitol (DTT), 2 % polyvinylpyrrolidone (PVP), and 1 mM phenylmethanesulfonyl fluoride (PMSF). The homogenate was centrifuged at 15,000*g* for 2 min, and the supernatant used immediately in the enzymatic assay. All extraction steps were performed at 4 °C.

PEPcase activity was estimated by NADH oxidation kinetics in the presence of malate dehydrogenase (MDH). The 100 μL extract was added to reaction medium composed by 100 mM HEPES-KOH buffer (pH 8.0) containing 5 mM $MgCl_2$, 2.5 mM phosphoenolpyruvate (PEP), 1 mM $NaHCO_3$, 0.2 mM NADH, and 5 U mL^{-1} malate dehydrogenase enzyme (MDH) at 30 °C. The reaction was monitored by absorbance decay at 340 nm. For each mol of malate produced is oxidized 1 mol of NADH, so the results were expressed as μmol NADH h^{-1} g^{-1} protein, using the NADH molar extinction coefficient (6.22 mM^{-1} cm^{-1}). Protein concentrations were determined by the Bradford method [33] by absorbance readings at 595 nm and using bovine serum albumin (Sigma-Aldrich, USA) as standard.

2.7. Chloroplast ultrastructure

For chloroplast ultrastructure, approximately 2 mm^2 leaf fragments from fully expanded leaves were fixed for 24 h in 50 mM phosphate buffer (pH 7.2) containing 2.5 % glutaraldehyde and 4 % paraformaldehyde. Subsequently, the material was rinsed three times in buffer and 45 min apart for each wash. Posteriorly, the samples were post-fixed with 1 % osmium tetroxide (OsO_4) in 50 mM phosphate buffer for 60 min and then rinsed again in the same buffer. The samples were then dehydrated with increasing series of 50 %, 70 %, 90 % and 100 % acetone for 45 min each step, and after infiltrated in epoxy resin (EMbed 812) according to the methodology described by Yamane et al. [34], with some modifications. The resin polymerization was performed at 60 °C. Ultrathin sections (70 nm) were placed on copper grids (300 mesh) and stained with 2 % uranyl acetate for 40 min, followed by 0.5 % lead citrate for 5 min. Finally, to generate chloroplast ultrastructure images, the sections were analyzed using a transmission electron microscope (JEOL JEM 1011) at 100 kV.

2.8. Metabolomic analysis

Extraction and derivatization of metabolites were performed as described by Lisec et al. [35], with adjustments. Approximately 50 mg of fully expanded leaf tissue (frozen) was macerated using liquid N_2 and homogenized with 100 % methanol (HPLC grade) containing ribitol (0.2 mg mL^{-1}) as a quantitative internal standard. The homogenate was incubated at 70 °C for 15 min under constant shaking. Then, the samples extracts were centrifuged at 12,000*g* for 10 min, and the supernatants were transferred to microtubes containing 100 % chloroform and ultrapure H_2O at 1:2 (v/v) ratio to separate polar and nonpolar phases inside the tubes. After vigorous vortexing, new centrifugation was conducted at 2,200*g* for 15 min. A 150 μL of the upper polar phase was carefully collected and transferred to another microtube. Samples were dehydrated and concentrated in vacuo system (SpeedVac Concentrator, Eppendorf, Hamburg, Germany), then stored at -80 °C. The metabolites were derivatized using 20 μL methoxyamine hydrochloride (20 mg mL^{-1} pyridin) for two hours at 37 °C. Subsequently with 35 μL *N*-methyl-*N*-(trimethylsilyl)trifluoroacetamide for 30 min at 37 °C.

Separation and identification of metabolites were performed according to Roessner et al. [36]. Samples were analyzed by a gas chromatography system coupled to mass spectrometry (GC–MS, QP-PLUS-2010, Shimadzu, Tokyo, Japan), using an RTX-5MS capillary column (30.0 m x0.25 mm x0.25 μm). A volume of 1 μL of each derivatized sample was injected with a split ratio of 1:5. The injection temperature was 250 °C, and helium carrier gas was at 1.2 mL min^{-1} constant flow rate. The temperature programming was as follows: 2 min at 80 °C, 10 °C min^{-1} ramp to 315 °C, and then held at 315 °C for 8 min. The transfer line and ion source were heated at 230 °C and 250 °C, respectively. Ionization was performed in an electron impact at 70 eV. The spectra in full scan mode were acquired from m/z 40 to 700. The solvent delay time was 3 min. Blank samples containing only derivatizing were done to identify possible contaminants.

Both chromatogram and mass spectral analysis were analyzed using the Xcalibur™ 2.1 software (Thermo Fisher Scientific, Waltham, MA, USA). All compounds were identified based on their retention times and mass spectrum fragmentation in comparison with an internal library composed by a mix of standards and its mass spectra previously identified based on the Golm Metabolome Database (GMD). The relative value of each metabolite was determined by the division of their respective peak areas by internal standard peak area (ribitol) and, after divided by the fresh weight of the sample.

2.9. Experimental design and statistical analysis

The experimental design was completely randomized, with a 2×2 factorial scheme. It was composed of two saline conditions [non-salt conditions (0 mM NaCl) and salt stress (80 mM NaCl)], and two leaf pretreatments [water-pretreated (0 mM H_2O_2) and H_2O_2-pretreated (10 mM H_2O_2)]. Each treatment was composed of four replicates consisting of two plants each. The physiological and biochemical data were submitted to a two-way analysis of variance (ANOVA), and the main values were compared by *F*-test ($p < 0.05$). Statistical analyses were performed using the Sisvar® 5.3 software. Also, these data were divided by the standard deviation of each variable (Autoscaling) for chemometrics analysis [PCA (Principal Component Analysis)] by MetabolAnalyst 4.0 (https://www.metaboanalyst.ca).

The relative values of metabolites were normalized by the control treatment and converted to $\log_2$ values to generate a Heatmap by MultiExperiment Viewer (MeV) 4.9 software. Besides, multivariate analysis was conducted log-transformed data by MetaboAnalyst 4.0. The transformed metabolic data were submitted to chemometrics analysis [PLS-DA (Partial Least Squares Discriminant Analysis)] and Variable Importance in Projection (VIP) scores, based on the first component of the PLS-DA model, was performed to identify potential biomarkers. Those metabolites with VIP > 1.3 were considered essential for treatment separation [37]. They were also submitted to a one-way ANOVA, and mean treatment values were separated by Tukey's test ($p < 0.05$). Besides, the log-transformed physiological, biochemical, and metabolic data were submitted to correlation analysis [Pearson correlation ($p < 0.05$)] by MetabolAnalyst 4.0.

3. Results

3.1. Gas exchange and chlorophyll parameters

H_2O_2 priming did not affect any gas exchange parameters of maize leaves in the absence of NaCl (Fig. 1). Conversely, salinity significantly reduced all gas exchange parameters of water-pretreated plants except for *A/Ci*, which increased by 20 %. Thus, *A*, *E,* and g_s rates decreased by 24 %, 21 %, and 48 %, respectively. However, foliar H_2O_2 priming was able to prevent damage caused by salt stress on *A* and *E*, although it did not attenuate the g_s reduction (Fig. 1a–c). Also, H_2O_2 priming increased the *A/Ci* ratio by 20 % under salt conditions (Fig. 1d). Salinity did not reduce the ΦPSII and ETR values; H_2O_2 priming nevertheless slightly increased these parameters under non-saline conditions (Table 1). Additionally, the salt stress reduced the Fv/Fm values by 18 %, but H_2O_2 priming decreased this reduction to 12 %. In contrast, salt stress increased NPQ by 115 %, and H_2O_2 primed plants under salt stress increased it more by 61 %, in comparison to only salt-stress treatment. While H_2O_2 priming and salinity single treatments equally increased qP values; however, no change occurred by the combined action of both treatments. Also, no significant difference in the photosynthetic pigments analyzed was perceived by H_2O_2 priming either in non-saline or saline conditions (Table 1). On the other hand, Chl *a*, Chl *b*, and Chl *total* contents decreased by 21, 58, and 42 %, respectively, under salt stress. Differently, carotenoid content was increased by 30 % under salt stress. Also, H_2O_2 priming did not significantly alter photosynthetic pigments under non-saline and saline conditions, except for an increase under non-saline conditions in the carotenoid content similar to that produced by saline stress.

3.2. Osmotic potential and reactive oxygen species

The H_2O_2 priming did not modify the Ψs of leaves under non-saline conditions, and the salinity reduced the Ψs by 32 % (Fig. 2a). However, H_2O_2 priming under salinity induced a further 24 % reduction of this value, in comparison to salt treatment alone. The H_2O_2 priming promoted an increase of 33 % in the $^{\bullet}O_2^-$ content but did not change H_2O_2 contents under non-saline conditions (Fig. 2b, c), and salinity promoted the growth of 26 and 36 % of $^{\bullet}O_2^-$ and H_2O_2 contents in water-pretreated plants, respectively. In contrast, H_2O_2 priming significantly reduced $^{\bullet}O_2^-$ and H_2O_2 contents in plants under salinity, making the values similar to those of water-pretreated plants without salt stress. The $^{\bullet}O_2^-$ and H_2O_2 reductions stimulated by H_2O_2 priming under salinity were 17 and 26 %, respectively, when compared to single salt treatment.

3.3. PEPcase activity and chloroplast ultrastructure

H_2O_2 priming reduced PEPcase activity in both the absence and presence of NaCl (Fig. 3). In contrast, salt treatment remarkably enhanced the enzyme activity, with an increase of 123 % in water-pretreated plants. However, H_2O_2 priming promoted a 52 % reduction of PEPcase activity under salinity. This decrease reached the value of PEPcase activity observed for water-pretreated plants without salinity. Also, the salinity caused damage in the mesophyll cells of maize leaves. In the absence of salinity, chloroplast ultrastructure exhibited a typical regular arrangement, characterized by well-stacked thylakoids and well-developed grana (Fig. 4a). The application of H_2O_2 priming apparently reduced the thylakoid stacking under non-salt conditions (Fig. 4b). Besides, salinity treatment promoted the unstacking and ripple in the thylakoid membranes (Fig. 4c). In contrast, the chloroplast of H_2O_2-pretreated plants under salt stress seemed to be like those of the water-pretreated plants under non-salt conditions, since it showed no abnormalities in their ultrastructure, as well as well-stacked thylakoid membranes (Fig. 4d).

3.4. PCA of physiological and biochemical data

According to PCA analysis gathering physiological and biochemical data, there was a clear separation between H_2O_2-pretreated and water-pretreated plants under both saline and non-saline conditions (Fig. 5a). However, the most evident separation was between the groups water-pretreated (S), and H_2O_2-pretreated (HS) plants both under salt stress. Also, between these two groups and the other two rest groups, water-pretreated (C) and H_2O_2-pretreated (H) plants both under non-salt conditions. The PCA showed that the first two components accounted for 72.8 % of the total variability. Loading plots showed the variation of each physiological and biochemical parameters (Fig. 5b). The first component (PC 1) was positively influenced by 8 of 17 parameters, and it was negatively affected by 9 of 17 parameters (Fig. 5b). Meanwhile, the second component (PC 2) was positively impacted by 10 of 17

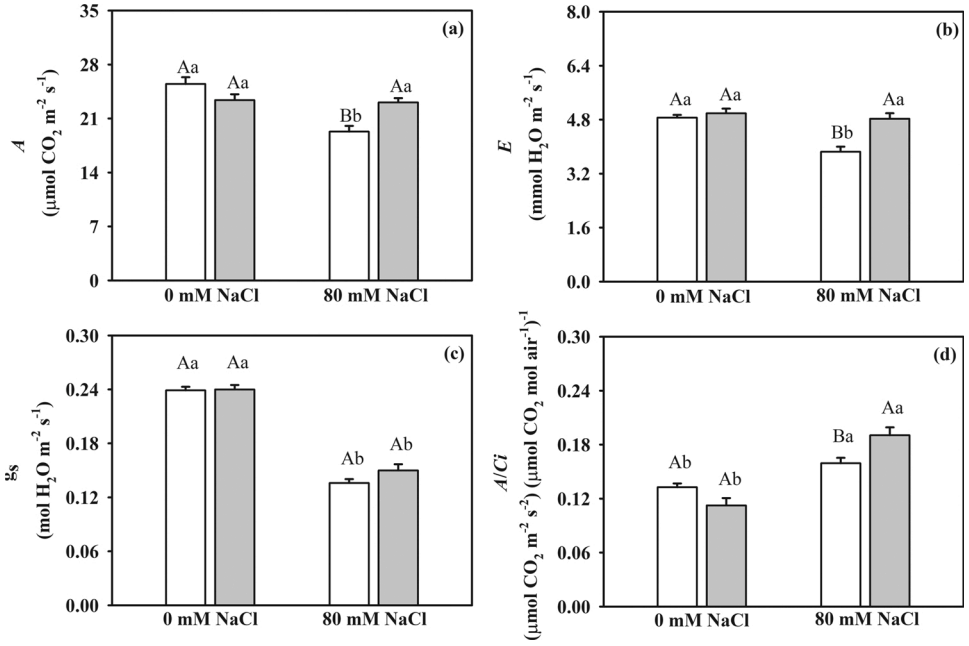

Fig. 1. Gas exchange measurements in the leaves of maize cv. BR 5011 water-pretreated (*white bars*) or H_2O_2-pretreated (*gray bars*) under non-salt conditions or salt stress conditions for twelve days. Rates of CO_2 assimilation (*A*, a), transpiration (*E*, b), stomatal conductance (g_s, c), and Rubisco carboxylation efficiency (*A/Ci*, d). For each variable, the capital letters and lowercase letters compare the H_2O_2 pretreatments and salinity treatments, respectively, according to *F*-test ($p < 0.05$). Error bars represent ± standard error and means represent $n = 5$.

Table 1
Chlorophyll *a* fluorescence parameters and photosynthetic pigments in leaves of maize cv. BR 5011 water-pretreated (C) or H_2O_2-pretreated (H) under non-salt conditions and water-pretreated (S) or H_2O_2-pretreated (HS) under salt stress conditions for twelve days. Values represent the means ($n = 5$) ± standard error.

Treatments	Chlorophyll *a* fluorescence variables [a]				
	ΦPSII [b]	Fv/Fm [b]	NPQ [b]	qP [b]	ETR
C	0.34 ± 0.01 Ba	0.61 ± 0.01 Aa	0.55 ± 0.08 Bb	0.56 ± 0.03 Bb	192.74 ± 9.07 Ba
H	0.39 ± 0.01 Aa	0.58 ± 0.01 Aa	0.70 ± 0.02 Ab	0.67 ± 0.01 Aa	204.44 ± 3.31 Aa
S	0.36 ± 0.00 Aa	0.50 ± 0.01 Bb	1.18 ± 0.03 Ba	0.71 ± 0.02 Aa	182.63 ± 2.52 Aa
HS	0.36 ± 0.02 Ab	0.54 ± 0.01 Ab	1.90 ± 0.08 Aa	0.67 ± 0.03 Aa	190.70 ± 3.08 Ab

Treatments	Photosynthetic pigments contents (μg g^{-1} DM) [a]			
	Chl *a*	Chl *b*	Chl *total*	Car [b]
C	373.7 ± 17.1 Aa	503.4 ± 29.8 Aa	877.1 ± 31.8 Aa	46.8 ± 4.9 Ab
H	385.6 ± 16.5 Aa	498.6 ± 14.7 Aa	884.2 ± 38.1 Aa	55.8 ± 5.5 Aa
S	294.4 ± 17.8 Ab	210.7 ± 11.1 Ab	505.9 ± 17.5 Ab	60.8 ± 1.7 Aa
HS	255.1 ± 11.2 Ab	313.8 ± 3.7 Ab	538.9 ± 23.2 Ab	49.3 ± 3.3 Aa

[a] For each variable, the capital letters and lowercase letters compare the H_2O_2 pretreatments and salinity treatments, respectively, according to *F*-test ($p < 0.05$).
[b] Significant interaction between treatments ($p < 0.05$).

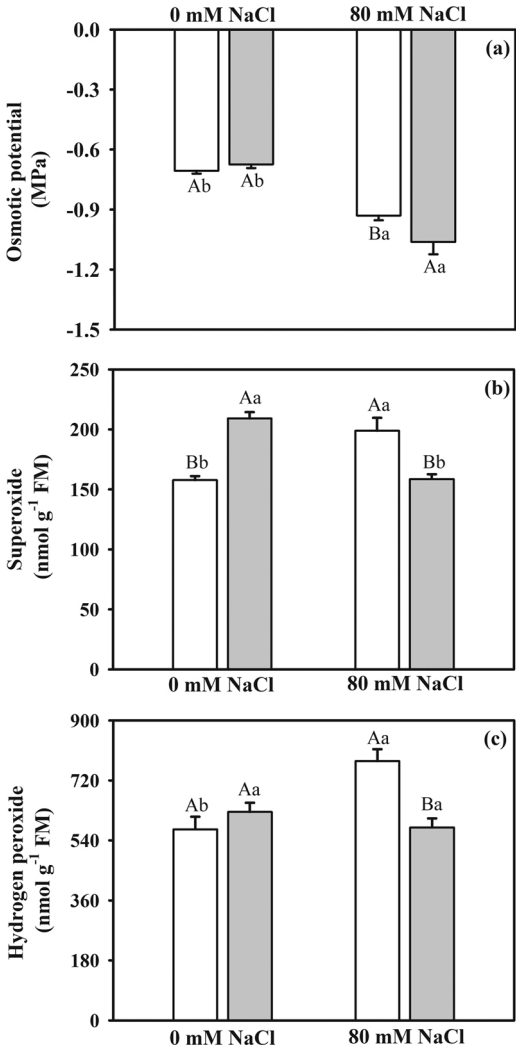

Fig. 2. Osmotic potential and reactive oxygen species in the leaves of maize cv. BR 5011 water-pretreated (*white bars*) or H_2O_2-pretreated (*gray bars*) under non-salt conditions or salt stress conditions for twelve days. Osmotic potential (a), and contents of superoxide radical (b) and hydrogen peroxide (c). For each variable, the capital letters and lowercase letters compare the H_2O_2 pretreatments and salinity treatments, respectively, according to *F*-test ($p < 0.05$). Error bars represent ± standard error and means represent $n = 5$.

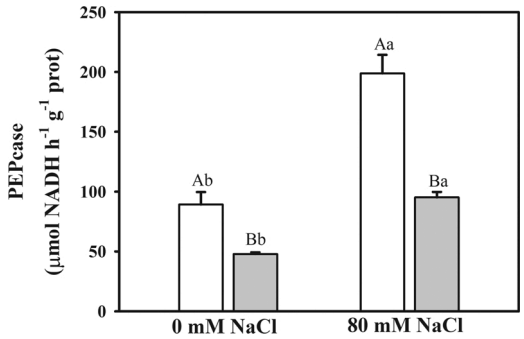

Fig. 3. Phosphoenolpyruvate carboxylase (PEPcase) activity in the leaves of maize cv. BR 5011 water-pretreated (*white bars*) or H_2O_2-pretreated (*gray bars*) under non-salt conditions or salt stress conditions for twelve days. The capital letters and lowercase letters compare the H_2O_2 pretreatments and salinity treatments, respectively, according to *F*-test ($p < 0.05$). Error bars represent ± standard error and means represent $n = 5$.

parameters, and it was negatively affected by 7 of 17 parameters.

3.5. Metabolomic profiling

Fifty-one compounds were identified in maize leaves (Tables S1 and S2). A heatmap also was built, showing the profile of each treatment normalized by the relative intensity values of the metabolites of water-pretreated plants under non-salt conditions, group C (Fig. 6). Carbohydrates, organic acids, and amino acids were the major compound groups classified. Twenty sugars and derivatives were detected, including erythritol, arabitol, ribulose-5-phosphate, galactinol, and raffinose, among others. Fourteen organic acids, including pyruvic acid, succinic acid, citric acid, and glyceric acid, among others, comprised the second major group. Ten amino acids and derivates were identified, including valine, serine, proline, asparagine, and tyrosine, among others. Finally, five phenolic compounds (shikimic acid, quinic acid, cinnamic acid, caffeic acid, and caffeoylquinic acid), and two nitrogenous compounds (uracil and spermine) were detected. In relative intensity terms, sucrose was the most predominant metabolite identified, followed by maleic acid, malonic acid, valine, and xylose. While aconitic acid, spermine, maltitol, uracil, and fumaric acid were among the five less predominant identified metabolites (Table S1).

In the absence of NaCl, H_2O_2 priming promoted a significant increase of six metabolites (maltitol, isomaltose, raffinose, lactic acid, asparagine, and quinic acid) and reduction three metabolites (xylitol, glutaric acid, and uracil) (Fig. 6; Table S1). Also, the salinity increased the relative intensity values of eight metabolites (glucose, ribulose-5-

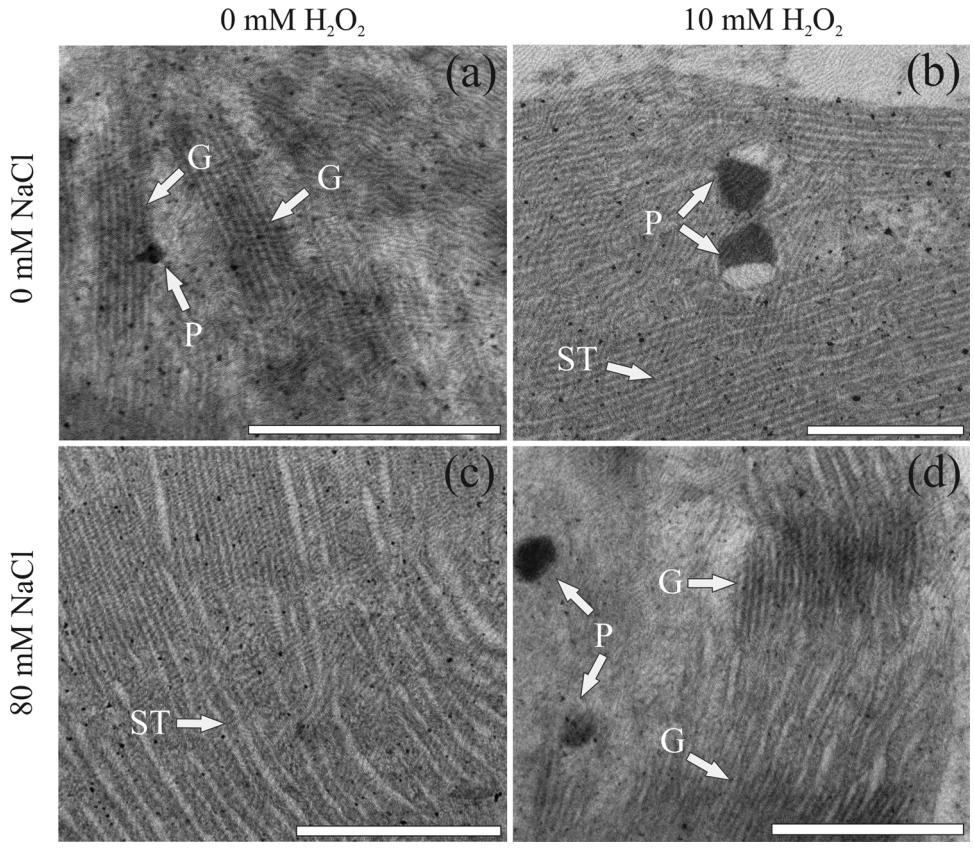

Fig. 4. Chloroplast ultrastructure by transmission electron microscopy in the mesophyll cells of maize cv. BR 5011 water-pretreated (a) or H_2O_2-pretreated (b) under non-salt conditions and water-pretreated (c) or H_2O_2-pretreated (d) under salt stress conditions for twelve days. G – grana; P – plastoglobule; ST – stromal thylakoids. Bars: 500 nm.

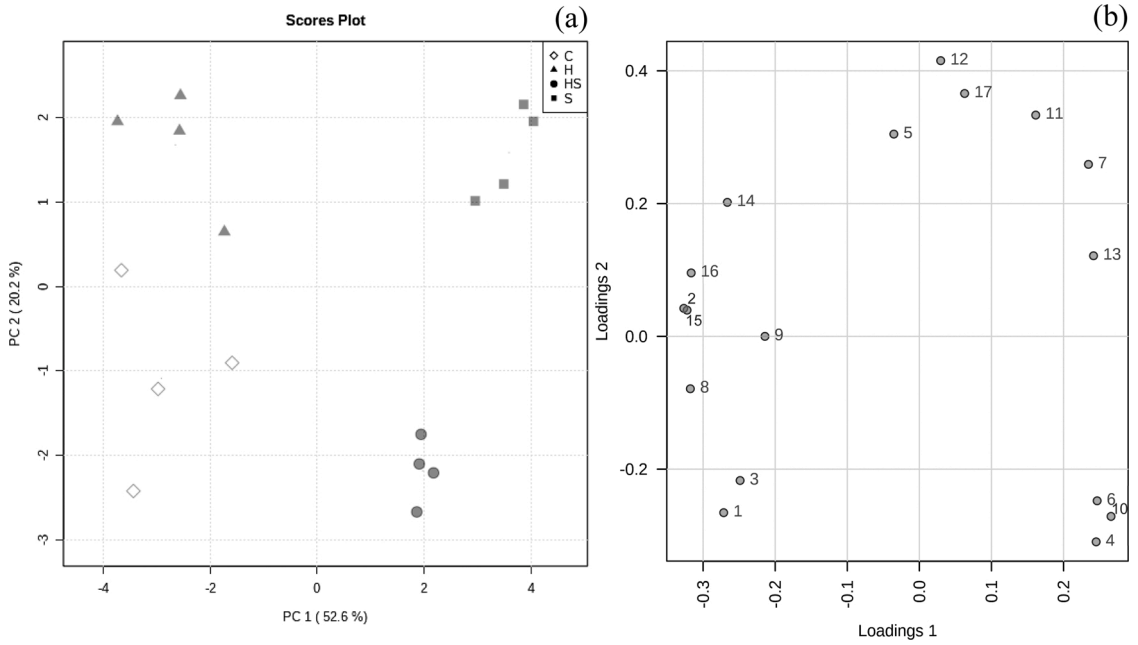

Fig. 5. Principal component analysis (PCA) of physiological and biochemical parameters in maize cv. BR 5011 water-pretreated (C) or H_2O_2-pretreated (H) under non-salt conditions and water-pretreated (S) or H_2O_2-pretreated (HS) under salt stress conditions for twelve days. Scores plot (a) and loading plot (b) of the first and second components (PC 1 and PC 2) indicating the clustering of samples into four groups. Paraments list: **1** CO_2 assimilation, **2** stomatal conductance, **3** transpiration, **4** carboxylation efficiency, **5** effective quantum yield of photosystem II, **6** non-photochemical quenching, **7** photochemical quenching, **8** photochemical quenching, **9** electron transport rate, **10** osmotic potential, **11** H_2O_2, **12** $\cdot O_2^-$, **13** PEPcase activity, **14** chlorophyll *a*, **15** chlorophyll *b*, **16** chlorophyll total, **17** carotenoids.

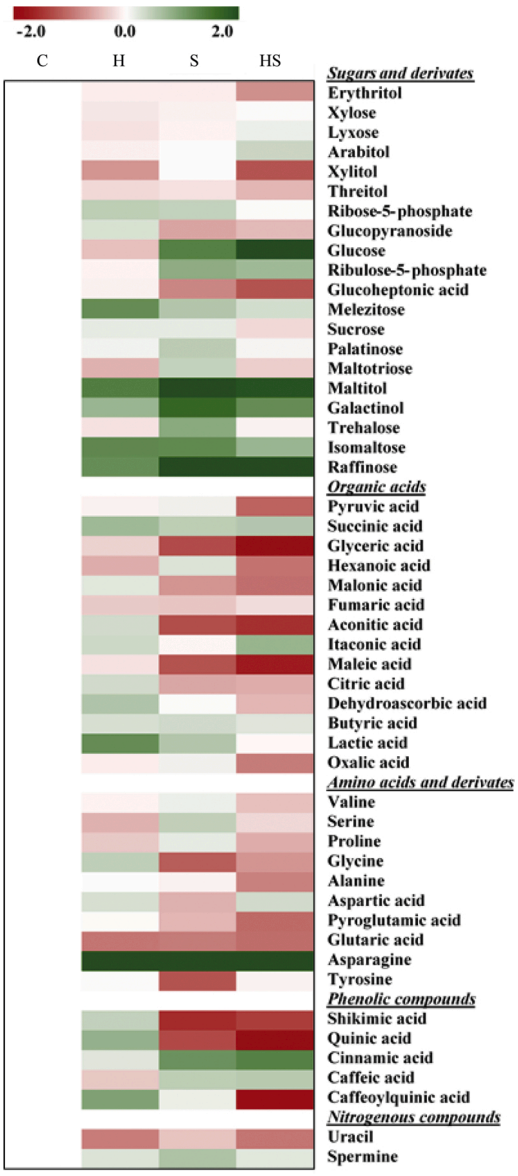

Fig. 6. Heat map of normalized values of metabolites in leaves of maize cv. BR 5011 water-pretreated (C) or H_2O_2-pretreated (H) under non-salt conditions and water-pretreated (S) or H_2O_2-pretreated (HS) under salt stress conditions for twelve days. The Heat map shows a high (green scale) or low (red scale) relative amount of each metabolite in comparison to control plants (uncolored scale). Each square represents the mean of four biological replicates, and the statistical difference was obtained according to *F*-test ($p < 0.05$). For more details, see Table S1. (For interpretation of the references to colour in this figure legend, the reader is referred to the web version of this article.)

phosphate, maltitol, galactinol, trehalose, raffinose, asparagine, and cinnamic acid), but it reduced other eleven metabolites (glucopyranoside, glucoheptonic acid, glyceric acid, malonic acid, aconitic acid, maleic acid, glycine, pyroglutamic acid, tyrosine, shikimic acid, and quinic acid) (Fig. 6; Table S1). Moreover, H_2O_2 priming altered the metabolic profile of maize leaves under salinity, increasing the relative intensity values of four metabolites (arabitol, glucose, asparagine, and tyrosine) when compared to water-pretreated plants under salinity (Fig. 6; Table S1). Conversely, H_2O_2 priming reduced other eleven metabolites, including sugars and derivates (erythritol, xylitol, trehalose, and raffinose), organic acids (pyruvic acid, glyceric acid, hexanoic acid, and oxalic acid), amino acid derivative (pyroglutamic acid), and phenolic compounds (quinic acid and caffeoylquinic acid).

The PLS-DA showed that the first two components accounted for 65.8 % of the total variability in maize leaves (Fig. 7a). Loading plots generated show the variation of individual metabolites in the experiment validates the PLS-DA (Fig. 7b). Besides, a cross-validation and permutation test ($p < 0.05$) allowed us to use PLS-DA instead of PCA analysis (Fig. 7c), which is more efficient to discriminate against the groups. It indicated a distinct separation of the four groups based only on the metabolic profiling of the treatments (Fig. 7a). Although the metabolite profile of water-pretreated and H_2O_2-pretreated plants without salinity showed proximity, they presented very distant of metabolite profile under salt stress, as shown by two-dimensional PLS-DA scores plot graph (Fig. 7a). Also, the loading plot graph showed metabolites responsible for the separation between groups observed in PLS-DA (Fig. 7b). The most positive contributing metabolites for the first component were raffinose, asparagine, glucose, maltitol cinnamic acid, and galactinol. In contrast, the most positive contributing metabolites for the second component were caffeoylquinic acid, lactic acid, pyruvic acid, and quinic acid (Fig. 7b). Besides, the variable importance in projection (VIP) *scores* graph displayed the most important metabolites for differentiating the treatments by the abundance of metabolites in each treatment (Fig. 8). VIP plot showed eleven metabolites of more than 1.3 VIP scores, in ascending order of VIP score they are: cinnamic acid, galactinol, maleic acid, aconitic acid, glyceric acid, glucose, shikimic acid, maltitol, quinic acid, asparagine, and raffinose (Fig. 8). Besides, among the 68 analyzed parameters, there are 71 positive correlations and 45 negative correlations with the Pearson coefficient greater than 0.8 (Table S3).

4. Discussion

4.1. H_2O_2 priming protects chloroplast ultrastructure and enhances photosynthetic machinery efficiency of maize leaves under salt stress

CO_2 assimilation is crucial for plant growth and development. It requires a photosynthetic apparatus that is particularly prepared to adjust to changes in environmental conditions. Therefore, simultaneous investigations of photosynthesis-related parameters from stomata to chloroplast allow a better understanding of salt effects and the priming action to minimize the damage involving environmental, biochemical, and morphological modulations [38]. Salt-stressed plants decrease their carbon assimilation capacity by displaying a reduction in gas exchange parameters and severe loss of photosynthetic pigments [39,40]. Our experimental results showed that salinity significantly reduced the gas exchange parameters, but there was an increase in *A/Ci* (Fig. 1). Despite the losses of carbon assimilation, the maize plant improves its carboxylation efficiency taking better advantage of the low concentration of CO_2 caused by stomatal closure by increasing the activity of PEPcase (Fig. 3). Besides, the salinity reduced Fv/Fm and an increase in NPQ and qP, indicating that the amount of energy absorbed not adequately transferred to reaction centers (Table 1). Indeed, the increase in NPQ was associated with heat dissipation in sunflower varieties sensitive to salinity even though it may not be sufficient to avoid damages [41].

The C4 plants use PEPcase in the CO_2 assimilation, improving photosynthetic performance, especially in a warm climate with high irradiance and low water availability, which can be significant benefits under other stress conditions too [42,43]. Also, the PEPcase has a non-photosynthetic role of replenishes intermediates of the citric acid cycle to nitrogen assimilation and multiple biosynthetic pathways [44, 45]. In this way, an increased PEPcase activity in response to abiotic stresses by an anaplerotic flow is expected [46]. It acts on defense and repair processes, such as biocompatible osmolytes biosynthesis and ROS detoxification [47]. Remarkably, maize plants invested in high PEPcase activity (Fig. 3), which reflected in the accumulation of sugars such as glucose, maltitol, raffinose, among others, in addition to the notable increase in asparagine (Fig. 6; Table S1). In contrast, the decrease of PEPcase activity in H_2O_2 pretreated plants under salinity led to levels

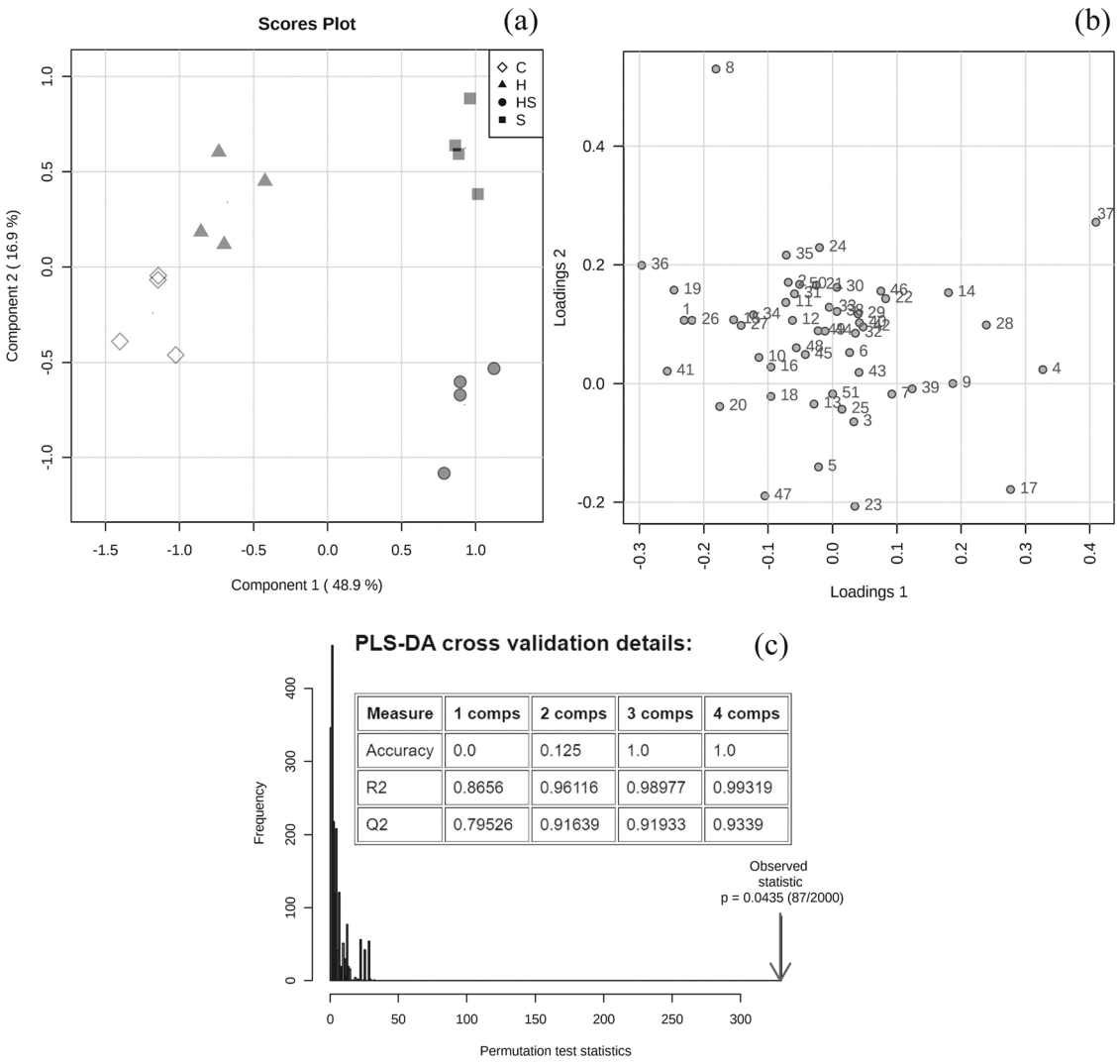

Fig. 7. Partial least squares - discriminant analysis (PLS-DA) of metabolic profiles in leaves of maize cv. BR 5011 water-pretreated (C) or H_2O_2-pretreated (H) under non-salt conditions and water-pretreated (S) or H_2O_2-pretreated (HS) under salt stress conditions for twelve days. Scores plot (a), loading plot (b), and PLS-DA cross-validation and permutation test (c) of the first and second components indicating the clustering of samples into four groups. Metabolites list: **1** Aconitic acid, **2** Alanine, **3** Arabitol, **4** Asparagine, **5** Aspartic acid, **6** Butyric acid, **7** Caffeic acid, **8** Caffeoylquinic acid, **9** Cinnamic acid, **10** Citric acid, **11** Dehydroascorbic acid, **12** Erythritol, **13** Fumaric acid, **14** Galactinol, **15** Glucoheptonic acid, **16** Glucopyranoside, **17** Glucose, **18** Glutaric acid, **19** Glyceric acid, **20** Glycine, **21** Hexanoic acid, **22** Isomaltose, **23** Itaconic acid, **24** Lactic acid, **25** Lyxose, **26** Maleic acid, **27** Malonic acid, **28** Maltitol, **29** Maltotriose, **30** Melezitose, **31** Oxalic acid, **32** Palatinose, **33** Proline, **34** Pyroglutamic acid, **35** Pyruvic acid, **36** Quinic acid, **37** Raffinose, **38** Ribose-5-phosphate, **39** Ribulose-5-phosphate, **40** Serine, **41** Shikimic acid, **42** Spermine, **43** Succinic acid, **44** Sucrose, **45** Threitol, **46** Trehalose, **47** Tyrosine, **48** Uracil, **49** Valine, **50** Xylitol, **51** Xylose.

close to those of control plants (Fig. 3). The H_2O_2 priming reduced the need for high PEPcase activity by re-calibrating PEPcase functions, allowing greater CO_2 assimilation and preserving high concentrations of ribulose-5-phosphate and glucose observed in maize leaves under salinity (Figs. 1, 6; Table S1).

The H_2O_2 priming improved Fv/Fm, as well as contributed to most of the excitation energy was dissipated in the form of NPQ without harming qP (Table 1). These effects of H_2O_2 priming can contribute to the normalization of *A* and *E* even under low g_s observed under salt stress, taking as reference water-pretreated plants under non-salt conditions (Fig. 1). Besides, the higher dissipation in the form of NPQ can contribute to less generation of ROS, mainly singlet oxygen [48]. Admittedly, the reduction of $^{\bullet}O_2^-$ and H_2O_2 in the leaves of H_2O_2-pretreated under salt conditions were notable (Fig. 2b, c). Thus, H_2O_2 priming improved the light energy conversion efficiency of PSII and carboxylation efficiency as well as minimized excess energy in PSII, which results in the improved photosynthetic performance of maize plants under salt stress (Fig. 1d, Table 1). Similar results were observed in mustard (*Brassica juncea* L.) seedlings, where the application of low concentrations of H_2O_2 increased photosynthesis due to an increase in Rubisco activity and PSII efficiency under abiotic stress [49].

Furthermore, the *Panax ginseng* and *Brassica napus* seedlings treated with exogenous H_2O_2 showed enhanced salinity tolerance due to decreasing of endogenous ROS contents, including both H_2O_2 and $^{\bullet}O_2^-$ [50,51]. Besides, salinity cause damages in the whole chloroplast ultrastructure, which is a reliable stress marker for plants during abiotic stress states [52]. Here, the structural changes were particularly prominent in thylakoids, that exhibited membrane undulations and granal unstacking (Fig. 4c). However, the exogenous H_2O_2 attenuated the effects of salt stress in maize chloroplast ultrastructure by reducing the oxidative stress generated by salinity by reducing of H_2O_2 and $^{\bullet}O_2^-$, so that practically no damage was observed in its ultrastructure (Figs. 2b, c and 4 d, h). Thus, our results reinforce the biochemical benefit of exogenous H_2O_2 in maize plants under salinity to alleviate salt-induced oxidative stress and protect the chloroplast structure against severe damage [53]. In this study, H_2O_2 priming, in addition to regulating the

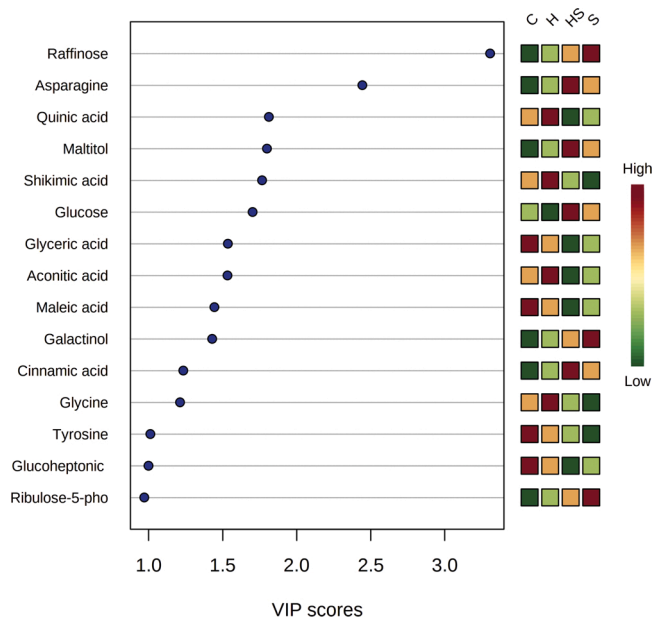

Fig. 8. VIP scores plot of metabolites in leaves of maize cv. BR 5011 water-pretreated (C) or H_2O_2-pretreated (H) under non-salt conditions and water-pretreated (S) or H_2O_2-pretreated (HS) under salt stress conditions for twelve days. The selected metabolites were those with a VIP score of greater than 1.0. Red or green squares on the right indicate the high and low abundance of the corresponding metabolite in each treatment, respectively. VIP score was based on the first component of the PLS-DA model. (For interpretation of the references to colour in this figure legend, the reader is referred to the web version of this article.)

ROS scavenging under salt stress, also induced metabolites of different metabolic and regulatory pathways like glucose, organic acids, amino acids, and polyphenols biosynthesis (Fig. 6, Table S1).

4.2. *Metabolomic profiling of H_2O_2-primed maize leaves reveals metabolites related to relief harmful effects of salt-stress*

The metabolomic approach used in this study allowed us to identify leaf metabolites modulated by maize plants in response to both H_2O_2 priming and salinity. Here, 42 metabolites among a total of 51 remained unchanged in H_2O_2-pretreated plants under non-salt conditions (Table S1), which was supported by a very similar physiological response profile influenced particularly by *A*, *E*, g_s, and photosynthetic pigments (Fig. 5). Recently, sprayed leaves with active priming compounds, such as jasmonates, salicylic acid, and methionine, were related to defense responses by the modulation of primary and secondary metabolite profiles to reduced plant water loss [54,55]. Although exogenous H_2O_2 slightly modified the metabolic profile of maize in the absence of salt, the accumulation of a few metabolites was noticeable (Table S1). Among them, the accumulation of quinic acid, a phenolic compound, biosynthesized by the shikimate pathway, in part, may contribute to adjusting H_2O_2 levels (Figs. 2c, 6). In fact, several priming compounds were all found to trigger the accumulation of quinic acids in tobacco cells [56], and it plays a role as an antioxidant agent acting in plant defense mechanisms and ROS scavenge [57]. Conversely, the presence of NaCl promoted considerable changes in the leaf metabolic profile of maize as increased in cinnamic acid previously reported in Thymus species in response to salinity [58]. However, the presence of salt negatively affected the accumulation of other endogenous phenolic compounds, as shikimic acid and quinic acid, which contribute reduce the antioxidant potential of plants increasing to the harmful effects observed [59]. Although, the beneficial of leaves pretreated with H_2O_2 under salinity could not link to these phenolic compounds identified here (Table S1).

In plants, carbohydrate metabolism is involved in crucial processes in response to abiotic stresses as well, playing a critical role in carbon storage, osmotic homeostasis, osmoprotectant, and free radicals elimination [60]. Our results showed that salinity increased six sugars and polyols (Fig. 6; Table S1). The hydroxyl groups of polyols can be replaced by water molecules and maintain hydrophilic interactions in plant cells, which are crucial for stabilizing macromolecules and membrane structure [60]. Indeed, carbohydrate stores are quickly mobilized, releasing soluble sugars that act as compatible solutes under stress [61]. Which, in part, supports the high levels of trehalose and raffinose under saline conditions. Such mechanism seems to be elicited in H_2O_2-pretreated plants under salt stress since the reduction of Ψs was accompanied by an increase in glucose and a significant decrease in these two polyols (Fig. 6; Table S1). Concurrently, the reduction of raffinose in the leaves can also be related to carbon export [62]. Furthermore, H_2O_2 priming also increased arabitol content, as well as in salt tolerant soy plants [63], and the gluconeogenesis process may be intensified by H_2O_2 priming since glucose values increased, and pyruvate values decreased (Fig. 6; Table S1) contributing to the mitigation of osmotic stress, which is a common phenomenon to promote tolerance to salt stress [64,65]. Another highlight is the increase of ribulose-5-phosphate under salinity conditions independently H_2O_2 priming (Fig. 6). It is a precursor on the ribulose-1,5-bisphosphate regeneration pathway, which does not necessarily indicate an inhibition of the carboxylation reaction as pointed out in C3 plants [66]. Once that H_2O_2-pretreated plants under salt stress showed recovery of *A* and high *A/Ci* in addition to normalization of PEPcase activity (Figs. 1a, d; 3).

Overall, the results here showed a decrease in some organic acids under salinity and H_2O_2 priming, particularly for some Krebs cycle intermediates and their precursors (aconitic acid and maleic acid), as well as glyceric acid, a metabolite involved in the glycolysis pathway. Such depletion is a remarkable metabolic characteristic observed in other plant species under salinity [67,68]. Besides, increased levels of the amino acid may be attributed to the induction of secondary metabolisms with increased levels of aromatic amino acids, such as tyrosine [69]. In this hand, an increase of asparagine is related to their role in transporting and storing nitrogen, as well as acts as a regulatory and signaling molecule of stress tolerance in plants [70]. Also, the increases in asparagine in sunflower leaves (*Helianthus annuus* L.) were related to mitigating the excess energy promoted by salinity [41].

Thus, plants under salt stress treatment only, and H_2O_2 pretreated plants under salinity presented differences in the modulation of sugars, as well as distinct adaptation mechanisms, displaying the complexity of carbohydrates in salinity tolerance. However, H_2O_2 priming provides a crucial role in minimizing the harmful effects of salt, because pretreated plants showed higher photosynthetic rates, reduced Ψs, maintenance of chloroplast ultrastructure, and reduced ROS even under salinity (Figs. 1–4).

5. Conclusion

Our study revealed some mechanisms alleviate harmful by salt stress by H_2O_2 priming. Also, it shows the four best salt stress biomarkers in maize leaves positively elicited by H_2O_2: raffinose, asparagine, quinic acid, and maltitol. The H_2O_2 priming was beneficial mainly by (i) inducing more efficient mechanisms to avoid salinity-induced energy excess, that could be attributed to maintaining high levels of photosynthetic pigments, elevated parameters of photochemical efficiency (Fv/Fm and NPQ), and regular PEPcase activity recovered; (ii) preserving the chloroplast ultrastructure by decrease both endogenous H_2O_2 and $^{\bullet}O_2^-$ contents; and (iii) regulate metabolites to the reestablishment of osmotic homeostasis and the scavenging of ROS.

Author agreement

All authors have read and approved the manuscript.

CRediT authorship contribution statement

Gyedre dos Santos Araújo: Conceptualization, Methodology, Formal analysis, Investigation, Data curation, Writing - original draft, Visualization. **Stelamaris de Oliveira Paula-Marinho:** Formal analysis, Investigation. **Sergimar Kennedy de Paiva Pinheiro:** Formal analysis. **Emílio de Castro Miguel:** Formal analysis. **Lineker de Sousa Lopes:** Data curation, Validation, Writing - review & editing. **Elton Camelo Marques:** Conceptualization. **Humberto Henrique de Carvalho:** Validation, Writing - review & editing. **Enéas Gomes-Filho:** Conceptualization, Validation, Resources, Supervision, Funding acquisition.

Declaration of Competing Interest

The authors report no declarations of interest.

Acknowledgments

This work was supported by the Conselho Nacional de Desenvolvimento Científico e Tecnológico (CNPq), the Coordenação de Aperfeiçoamento de Pessoal de Nível Superior (CAPES), the Fundação Cearense de Apoio ao Desenvolvimento Científico e Tecnológico (FUNCAP) and Central Analítica-UFC/CT-INFRA/MCTI-SISANO/Pró-Equipamentos CAPES.

Appendix A. Supplementary data

Supplementary material related to this article can be found, in the online version, at doi:https://doi.org/10.1016/j.plantsci.2020.110774.

References

[1] R.S. Sekhon, M.W. Breitzman, R.R. Silva, N. Santoro, W.L. Rooney, N. de Leon, S. M. Kaeppler, Stover composition in maize and sorghum reveals remarkable genetic variation and plasticity for carbohydrate accumulation, Front. Plant Sci. 7 (2016), https://doi.org/10.3389/fpls.2016.00822.

[2] Statistics | Food and Agriculture Organization of the United Nations, FAO, 2019 (Accessed 3 December 2019), http://www.fao.org/statistics/en.

[3] A. EL Sabagh, A. Hossain, M. Aamir Iqbal, C. Barutçular, M.S. Islam, F. Çiğ, M. Erman, O. Sytar, M. Brestic, A. Wasaya, T. Jabeen, M. Asif Bukhari, M. Mubeen, H.-R. Athar, F. Azeem, H. Akdeniz, Ö. Konuşkan, F. Kizilgeci, M. Ikram, S. Sorour, W. Nasim, M. Elsabagh, M. Rizwan, R. Swaroop Meena, S. Fahad, A. Ueda, L. Liu, H. Saneoka, Maize adaptability to heat stress under changing climate. Plant Stress Physiol., IntechOpen, 2020, https://doi.org/10.5772/intechopen.92396 [Working Title].

[4] P. Li, W. Cao, H. Fang, S. Xu, S. Yin, Y. Zhang, D. Lin, J. Wang, Y. Chen, C. Xu, Z. Yang, Transcriptomic profiling of the maize (Zea mays L.) leaf response to abiotic stresses at the seedling stage, Front. Plant Sci. 8 (2017), https://doi.org/10.3389/fpls.2017.00290.

[5] F.K. Choudhury, R.M. Rivero, E. Blumwald, R. Mittler, Reactive oxygen species, abiotic stress and stress combination, Plant J. 90 (2017) 856–867, https://doi.org/10.1111/tpj.13299.

[6] S.V. Isayenkov, F.J.M. Maathuis, Plant salinity stress: many unanswered questions remain, Front. Plant Sci. 10 (2019) 80, https://doi.org/10.3389/fpls.2019.00080.

[7] R. Borges, E.C. Miguel, J.M.R. Dias, M. da Cunha, R.E. Bressan-Smith, J.G. de Oliveira, G.A. de Souza Filho, Ultrastructural, physiological and biochemical analyses of chlorate toxicity on rice seedlings, Plant Sci. 166 (2004) 1057–1062, https://doi.org/10.1016/j.plantsci.2003.12.023.

[8] C. Huang, G. Wei, Y. Jie, L. Wang, H. Zhou, C. Ran, Z. Huang, H. Jia, S.A. Anjum, Effects of concentrations of sodium chloride on photosynthesis, antioxidative enzymes, growth and fiber yield of hybrid ramie, Plant Physiol. Biochem. 76 (2014) 86–93, https://doi.org/10.1016/j.plaphy.2013.12.021.

[9] A. Abdelraheem, N. Esmaeili, M. O'Connell, J. Zhang, Progress and perspective on drought and salt stress tolerance in cotton, Ind. Crops Prod. 130 (2019) 118–129, https://doi.org/10.1016/j.indcrop.2018.12.070.

[10] M. Singh, A. Singh, S.M. Prasad, R.K. Singh, Regulation of plants metabolism in response to salt stress: an omics approach, Acta Physiol. Plant. 39 (2017) 48, https://doi.org/10.1007/s11738-016-2345-x.

[11] P. Filippou, G. Tanou, A. Molassiotis, V. Fotopoulos, Plant acclimation to environmental stress using priming agents. Plant Acclim. to Environ. Stress, Springer, New York, New York, NY, 2013, pp. 1–27, https://doi.org/10.1007/978-1-4614-5001-6_1.

[12] A. Savvides, S. Ali, M. Tester, V. Fotopoulos, Chemical priming of plants against multiple abiotic stresses: mission possible? Trends Plant Sci. 21 (2016) 329–340, https://doi.org/10.1016/j.tplants.2015.11.003.

[13] C. González-Bosch, Priming plant resistance by activation of redox-sensitive genes, Free Radic. Biol. Med. 122 (2018) 171–180, https://doi.org/10.1016/j.freeradbiomed.2017.12.028.

[14] M.A. Ashraf, A. Akbar, S.H. Askari, M. Iqbal, R. Rasheed, I. Hussain, Recent advances in abiotic stress tolerance of plants through chemical priming: an overview. Adv. Seed Priming, Springer, Singapore, Singapore, 2018, pp. 51–79, https://doi.org/10.1007/978-981-13-0032-5_4.

[15] M. Thakur, P. Sharma, A. Anand, Seed priming-induced early vigor in crops: an alternate strategy for abiotic stress tolerance. Priming Pretreat. Seeds Seedlings, Springer, Singapore, Singapore, 2019, pp. 163–180, https://doi.org/10.1007/978-981-13-8625-1_8.

[16] A. Singh, A. Kumar, S. Yadav, I.K. Singh, Reactive oxygen species-mediated signaling during abiotic stress, Plant Gene 18 (2019) 100173, https://doi.org/10.1016/j.plgene.2019.100173.

[17] T.A. Khan, M. Yusuf, Q. Fariduddin, Hydrogen peroxide in regulation of plant metabolism: signalling and its effect under abiotic stress, Photosynthetica 56 (2018) 1237–1248, https://doi.org/10.1007/s11099-018-0830-8.

[18] Y. Gao, Y.-K. Guo, S.-H. Lin, Y.-Y. Fang, J.-G. Bai, Hydrogen peroxide pretreatment alters the activity of antioxidant enzymes and protects chloroplast ultrastructure in heat-stressed cucumber leaves, Sci. Hortic. (Amst.) 126 (2010) 20–26, https://doi.org/10.1016/j.scienta.2010.06.006.

[19] F.A. Gondim, E. Gomes-Filho, J.H. Costa, N.L.M. Alencar, J.T. Prisco, Catalase plays a key role in salt stress acclimation induced by hydrogen peroxide pretreatment in maize, Plant Physiol. Biochem. 56 (2012) 62–71, https://doi.org/10.1016/j.plaphy.2012.04.012.

[20] F.A. Gondim, R.S. Miranda, E. Gomes-Filho, J.T. Prisco, Enhanced salt tolerance in maize plants induced by H2O2 leaf spraying is associated with improved gas exchange rather than with non-enzymatic antioxidant system, Theor. Exp. Plant Physiol. 25 (2013) 251–260, https://doi.org/10.1590/S2197-00252013000400003.

[21] M. Debnath, N. Ashwath, C.B. Hill, D.L. Callahan, D.A. Dias, N.S. Jayasinghe, D. J. Midmore, U. Roessner, Comparative metabolic and ionomic profiling of two cultivars of Stevia rebaudiana Bert. (Bertoni) grown under salinity stress, Plant Physiol. Biochem. 129 (2018) 56–70, https://doi.org/10.1016/j.plaphy.2018.05.001.

[22] Y. Wang, X. Zeng, Q. Xu, X. Mei, H. Yuan, D. Jiabu, Z. Sang, T. Nyima, Metabolite profiling in two contrasting Tibetan hulless barley cultivars revealed the core salt-responsive metabolome and key salt-tolerance biomarkers, AoB Plants 11 (2019), https://doi.org/10.1093/aobpla/plz021.

[23] A. Llanes, A. Andrade, S. Alemano, V. Luna, Metabolomic approach to understand plant adaptations to water and salt stress. Plant Metab. Regul. Under Environ. Stress, Elsevier, 2018, pp. 133–144, https://doi.org/10.1016/B978-0-12-812689-9.00006-6.

[24] A.D. de Azevedo Neto, J.T. Prisco, J. Enéas-Filho, C.F. de Lacerda, J.V. Silva, P.H. A. da Costa, E. Gomes-Filho, Effects of salt stress on plant growth, stomatal response and solute accumulation of different maize genotypes, Braz. J. Plant Physiol. 16 (2004) 31–38, https://doi.org/10.1590/S1677-04202004000100005.

[25] D.R. Hoagland, D.I. Arnon, The water-culture method for growing plants without soil, Circ. Calif. Agric. Exp. Stn. 347 (1950).

[26] W. Bilger, U. Schreiber, M. Bock, Determination of the Quantum Efficiency of Photosystem II and of Non-Photochemical Quenching of Chlorophyll Fluorescence in the Field, Springer-Verlag, 1995.

[27] A.N. Callister, S.K. Arndt, M.A. Adams, Comparison of four methods for measuring osmotic potential of tree leaves, Physiol. Plant. 127 (2006) 383–392, https://doi.org/10.1111/j.1399-3054.2006.00652.x.

[28] A.R. Wellburn, The spectral determination of chlorophylls a and b, as well as total carotenoids, using various solvents with spectrophotometers of different resolution, J. Plant Physiol. 144 (1994) 307–313, https://doi.org/10.1016/S0176-1617(11)81192-2.

[29] J.M. Cheeseman, Hydrogen peroxide concentrations in leaves under natural conditions, J. Exp. Bot. 57 (2006) 2435–2444, https://doi.org/10.1093/jxb/erl004.

[30] C.D. Fernando, P. Soysa, Optimized enzymatic colorimetric assay for determination of hydrogen peroxide (H2O2) scavenging activity of plant extracts, MethodsX 2 (2015) 283–291, https://doi.org/10.1016/j.mex.2015.05.001.

[31] A. Klein, L. Hüsselmann, M. Keyster, N. Ludidi, Exogenous nitric oxide limits salt-induced oxidative damage in maize by altering superoxide dismutase activity, S. Afr. J. Bot. 115 (2018) 44–49, https://doi.org/10.1016/j.sajb.2017.12.010.

[32] C. Echevarria, V. Pacquit, N. Bakrim, L. Osuna, B. Delgado, M. Arriodupont, J. Vidal, The effect of pH on the covalent and metabolic control of C4 phosphoenolpyruvate carboxylase from Sorghum leaf, Arch. Biochem. Biophys. 315 (1994) 425–430, https://doi.org/10.1006/abbi.1994.1520.

[33] M.M. Bradford, A rapid and sensitive method for the quantitation of microgram quantities of protein utilizing the principle of protein-dye binding, Anal. Biochem. 72 (1976) 248–254, https://doi.org/10.1016/0003-2697(76)90527-3.

[34] K. Yamane, S. Mitsuya, M. Taniguchi, H. Miyake, Salt-induced chloroplast protrusion is the process of exclusion of ribulose-1,5-bisphosphate carboxylase/oxygenase from chloroplasts into cytoplasm in leaves of rice, Plant Cell Environ. 35 (2012) 1663–1671, https://doi.org/10.1111/j.1365-3040.2012.02516.x.

[35] J. Lisec, N. Schauer, J. Kopka, L. Willmitzer, A.R. Fernie, Gas chromatography mass spectrometry–based metabolite profiling in plants, Nat. Protoc. 1 (2006) 387–396, https://doi.org/10.1038/nprot.2006.59.
[36] U. Roessner, A. Luedemann, D. Brust, O. Fiehn, T. Linke, L. Willmitzer, A.R. Fernie, Metabolic Profiling Allows Comprehensive Phenotyping of Genetically or Environmentally Modified Plant Systems, 2001 (Accessed 7 July 2020), www.plantcell.org.
[37] J. Xia, I.V. Sinelnikov, B. Han, D.S. Wishart, MetaboAnalyst 3.0—making metabolomics more meaningful, Nucleic Acids Res. 43 (2015) W251–W257, https://doi.org/10.1093/nar/gkv380.
[38] H.M. Kalaji, A. Jajoo, A. Oukarroum, M. Brestic, M. Zivcak, I.A. Samborska, M. D. Cetner, I. Łukasik, V. Goltsev, R.J. Ladle, Chlorophyll *a* fluorescence as a tool to monitor physiological status of plants under abiotic stress conditions, Acta Physiol. Plant. 38 (2016), https://doi.org/10.1007/s11738-016-2113-y.
[39] R. de S. Miranda, R.O. Mesquita, N.S. Freitas, J.T. Prisco, E. Gomes-Filho, Nitrate: ammonium nutrition alleviates detrimental effects of salinity by enhancing photosystem II efficiency in sorghum plants, Rev. Bras. Eng. Agríc. Ambient. 18 (2014) 8–12, https://doi.org/10.1590/1807-1929/agriambi.v18nsupps8-s12.
[40] R. Sozharajan, S. Natarajan, NaCl stress causes changes in photosynthetic pigments and accumulation of compatible solutes in Zea mays L, J. Appl. Adv. Res. 1 (2016) 3, https://doi.org/10.21839/jaar.2016.v1i1.6.
[41] G. dos S. Araújo, R. de S. Miranda, R.O. Mesquita, S. de O. Paula, J.T. Prisco, E. Gomes-Filho, Nitrogen assimilation pathways and ionic homeostasis are crucial for photosynthetic apparatus efficiency in salt-tolerant sunflower genotypes, Plant Growth Regul. 86 (2018) 375–388, https://doi.org/10.1007/s10725-018-0436-y.
[42] R.F. Sage, The evolution of C4 photosynthesis, New Phytol. 161 (2004) 341–370, https://doi.org/10.1111/j.1469-8137.2004.00974.x.
[43] V. Doubnerová, H. Ryšlavá, What can enzymes of C4 photosynthesis do for C3 plants under stress? Plant Sci. 180 (2011) 575–583, https://doi.org/10.1016/j.plantsci.2010.12.005.
[44] J. Shi, K. Yi, Y. Liu, L. Xie, Z. Zhou, Y. Chen, Z. Hu, T. Zheng, R. Liu, Y. Chen, J. Chen, Phospho enol pyruvate carboxylase in Arabidopsis leaves plays a crucial role in carbon and nitrogen metabolism, Plant Physiol. 167 (2015) 671–681, https://doi.org/10.1104/pp.114.254474.
[45] M. Waseem, F. Ahmad, The phosphoenolpyruvate carboxylase gene family identification and expression analysis under abiotic and phytohormone stresses in Solanum lycopersicum L, Gene 690 (2019) 11–20, https://doi.org/10.1016/j.gene.2018.12.033.
[46] V.D. Hýsková, L. Miedzińska, J. Dobrá, R. Vankova, H. Ryšlavá, Phosphoenolpyruvate carboxylase, NADP-malic enzyme, and pyruvate, phosphate dikinase are involved in the acclimation of Nicotiana tabacum L. to drought stress, J. Plant Physiol. 171 (2014) 19–25, https://doi.org/10.1016/j.jplph.2013.10.017.
[47] N. Wang, X. Zhong, Y. Cong, T. Wang, S. Yang, Y. Li, J. Gai, Genome-wide analysis of phosphoenolpyruvate carboxylase gene family and their response to abiotic stresses in soybean, Sci. Rep. 6 (2016) 38448, https://doi.org/10.1038/srep38448.
[48] P. Müller, X.-P. Li, K.K. Niyogi, Non-photochemical quenching. A response to excess light energy, Plant Physiol. 125 (2001) 1558–1566, https://doi.org/10.1104/pp.125.4.1558.
[49] H.A. Khan, K.H.M. Siddique, R. Munir, T.D. Colmer, Salt sensitivity in chickpea: growth, photosynthesis, seed yield components and tissue ion regulation in contrasting genotypes, J. Plant Physiol. 182 (2015) 1–12, https://doi.org/10.1016/j.jplph.2015.05.002.
[50] G. Sathiyaraj, S. Srinivasan, Y.-J. Kim, O.R. Lee, S. Parvin, S.R.D. Balusamy, A. Khorolragchaa, D.C. Yang, Acclimation of hydrogen peroxide enhances salt tolerance by activating defense-related proteins in Panax ginseng C.A. Meyer, Mol. Biol. Rep. 41 (2014) 3761–3771, https://doi.org/10.1007/s11033-014-3241-3.
[51] M. Hasanuzzaman, K. Nahar, S.S. Gill, H.F. Alharby, B.H.N. Razafindrabe, M. Fujita, Hydrogen peroxide pretreatment mitigates cadmium-induced oxidative stress in Brassica napus L.: an intrinsic study on antioxidant defense and glyoxalase systems, Front. Plant Sci. 8 (2017), https://doi.org/10.3389/fpls.2017.00115.
[52] B. Zechmann, Ultrastructure of plastids serves as reliable abiotic and biotic stress marker, PLoS One 14 (2019) e0214811, https://doi.org/10.1371/journal.pone.0214811.
[53] J. Shen, Y. Wang, S. Shu, M.S. Jahan, M. Zhong, J. Wu, J. Sun, S. Guo, Exogenous putrescine regulates leaf starch overaccumulation in cucumber under salt stress, Sci. Hortic. (Amst.) 253 (2019) 99–110, https://doi.org/10.1016/j.scienta.2019.04.010.
[54] V.C.V. Batista, I.M.C. Pereira, S. de O. Paula-Marinho, K.M. Canuto, R. de C.A. Pereira, T.H.S. Rodrigues, D. de M. Daloso, E. Gomes-Filho, H.H. de Carvalho, Salicylic acid modulates primary and volatile metabolites to alleviate salt stress-induced photosynthesis impairment on medicinal plant Egletes viscosa, Environ. Exp. Bot. 167 (2019) 103870, https://doi.org/10.1016/j.envexpbot.2019.103870.
[55] I. Hassini, J.J. Rios, P. Garcia-Ibañez, N. Baenas, M. Carvajal, D.A. Moreno, Comparative effect of elicitors on the physiology and secondary metabolites in broccoli plants, J. Plant Physiol. 239 (2019) 1–9, https://doi.org/10.1016/j.jplph.2019.05.008.
[56] M.I. Mhlongo, P.A. Steenkamp, L.A. Piater, N.E. Madala, I.A. Dubery, Profiling of altered metabolomic states in Nicotiana tabacum cells induced by priming agents, Front. Plant Sci. 7 (2016) 1527, https://doi.org/10.3389/fpls.2016.01527.
[57] T. Isah, Stress and defense responses in plant secondary metabolites production, Biol. Res. 52 (2019) 39, https://doi.org/10.1186/s40659-019-0246-3.
[58] Z.E. Bistgani, M. Hashemi, M. DaCosta, L. Craker, F. Maggi, M.R. Morshedloo, Effect of salinity stress on the physiological characteristics, phenolic compounds and antioxidant activity of Thymus vulgaris L. and thymus daenensis celak, Ind. Crops Prod. 135 (2019) 311–320, https://doi.org/10.1016/j.indcrop.2019.04.055.
[59] A. Sharma, B. Shahzad, A. Rehman, R. Bhardwaj, M. Landi, B. Zheng, Response of phenylpropanoid pathway and the role of polyphenols in plants under abiotic stress, Molecules 24 (2019) 2452, https://doi.org/10.3390/molecules24132452.
[60] M.P. Gangola, B.R. Ramadoss, Sugars play a critical role in abiotic stress tolerance in plants. Biochem. Physiol. Mol. Ave. Combat. Abiotic Stress Plants, Elsevier, 2018, pp. 17–38, https://doi.org/10.1016/B978-0-12-813066-7.00002-4.
[61] G.M. Borrelli, M. Fragasso, F. Nigro, C. Platani, R. Papa, R. Beleggia, D. Trono, Analysis of metabolic and mineral changes in response to salt stress in durum wheat (Triticum turgidum ssp. durum) genotypes, which differ in salinity tolerance, Plant Physiol. Biochem. 133 (2018) 57–70, https://doi.org/10.1016/j.plaphy.2018.10.025.
[62] S. Sengupta, S. Mukherjee, P. Basak, A.L. Majumder, Significance of galactinol and raffinose family oligosaccharide synthesis in plants, Front. Plant Sci. 6 (2015) 656, https://doi.org/10.3389/fpls.2015.00656.
[63] Y. Jiao, Z. Bai, J. Xu, M. Zhao, Y. Khan, Y. Hu, L. Shi, Metabolomics and its physiological regulation process reveal the salt-tolerant mechanism in Glycine soja seedling roots, Plant Physiol. Biochem. 126 (2018) 187–196, https://doi.org/10.1016/j.plaphy.2018.03.002.
[64] X. Guo, Y. Wang, H. Lu, X. Cai, X. Wang, Z. Zhou, C. Wang, Y. Wang, Z. Zhang, K. Wang, F. Liu, Genome-wide characterization and expression analysis of the aldehyde dehydrogenase (ALDH) gene superfamily under abiotic stresses in cotton, Gene 628 (2017) 230–245, https://doi.org/10.1016/j.gene.2017.07.034.
[65] P. Poór, Z. Czékus, A. Ördög, Role and regulation of glucose as a signal molecule to Salt stress. Plant Signal. Mol., Elsevier, 2019, pp. 193–205, https://doi.org/10.1016/B978-0-12-816451-8.00012-5.
[66] M.S. Hossain, M. Persicke, A.I. ElSayed, J. Kalinowski, K.-J. Dietz, Metabolite profiling at the cellular and subcellular level reveals metabolites associated with salinity tolerance in sugar beet, J. Exp. Bot. 68 (2017) 5961–5976, https://doi.org/10.1093/jxb/erx388.
[67] D.H. Sanchez, F. Lippold, H. Redestig, M.A. Hannah, A. Erban, U. Krämer, J. Kopka, M.K. Udvardi, Integrative functional genomics of salt acclimatization in the model legume Lotus japonicus, Plant J. 53 (2007) 973–987, https://doi.org/10.1111/j.1365-313X.2007.03381.x.
[68] J.A. Richter, A. Erban, J. Kopka, C. Zörb, Metabolic contribution to salt stress in two maize hybrids with contrasting resistance, Plant Sci. 233 (2015) 107–115, https://doi.org/10.1016/j.plantsci.2015.01.006.
[69] X.L. Zhang, X.F. Jia, B. Yu, Y. Gao, J.G. Bai, Exogenous hydrogen peroxide influences antioxidant enzyme activity and lipid peroxidation in cucumber leaves at low light, Sci. Hortic. (Amst.) 129 (2011) 656–662, https://doi.org/10.1016/j.scienta.2011.05.009.
[70] L. Gaufichon, M. Reisdorf-Cren, S.J. Rothstein, F. Chardon, A. Suzuki, Biological functions of asparagine synthetase in plants, Plant Sci. 179 (2010) 141–153, https://doi.org/10.1016/j.plantsci.2010.04.010.